Development and Psychopathology **31** (2019), 557–571

doi:10.1017/S0954579418000093

Brain structural covariance network centrality in maltreated youth with PTSD and in maltreated youth resilient to PTSD

DELIN SUN,[a,b] COURTNEY C. HASWELL,[a,b] RAJENDRA A. MOREY,[a,b,c] AND MICHAEL D. DE BELLIS[a,c]
[a]*Duke University;* [b]*Mid-Atlantic Mental Illness Research and Clinical Center; and* [c]*Duke University School of Medicine*

Abstract

Child maltreatment is a major cause of pediatric posttraumatic stress disorder (PTSD). Previous studies have not investigated potential differences in network architecture in maltreated youth with PTSD and those resilient to PTSD. High-resolution magnetic resonance imaging brain scans at 3 T were completed in maltreated youth with PTSD ($n = 31$), without PTSD ($n = 32$), and nonmaltreated controls ($n = 57$). Structural covariance network architecture was derived from between-subject intraregional correlations in measures of cortical thickness in 148 cortical regions (nodes). Interregional positive partial correlations controlling for demographic variables were assessed, and those correlations that exceeded specified thresholds constituted connections in cortical brain networks. Four measures of network centrality characterized topology, and the importance of cortical regions (nodes) within the network architecture were calculated for each group. Permutation testing and principle component analysis method were employed to calculate between-group differences. Principle component analysis is a methodological improvement to methods used in previous brain structural covariance network studies. Differences in centrality were observed between groups. Larger centrality was found in maltreated youth with PTSD in the right posterior cingulate cortex; smaller centrality was detected in the right inferior frontal cortex compared to youth resilient to PTSD and controls, demonstrating network characteristics unique to pediatric maltreatment-related PTSD. Larger centrality was detected in right frontal pole in maltreated youth resilient to PTSD compared to youth with PTSD and controls, demonstrating structural covariance network differences in youth resilience to PTSD following maltreatment. Smaller centrality was found in the left posterior cingulate cortex and in the right inferior frontal cortex in maltreated youth compared to controls, demonstrating attributes of structural covariance network topology that is unique to experiencing maltreatment. This work is the first to identify cortical thickness-based structural covariance network differences between maltreated youth with and without PTSD. We demonstrated network differences in both networks unique to maltreated youth with PTSD and those resilient to PTSD. The networks identified are important for the successful attainment of age-appropriate social cognition, attention, emotional processing, and inhibitory control. Our findings in maltreated youth with PTSD versus those without PTSD suggest vulnerability mechanisms for developing PTSD.

Keywords: cortical networks; cortical thickness; maltreatment; network centrality; pediatric PTSD; resilience

Child maltreatment is a public health problem associated with alterations in trajectories of brain development (Teicher, Samson, Anderson, & Ohashi, 2016), significant psychopathology (Kim & Cicchetti, 2010), and high rates of pediatric posttraumatic stress disorder (PTSD; De Bellis, 2001; De Bellis & Zisk, 2014). There is a paucity of brain imaging studies that examine maltreated youth with PTSD versus those resilient to PTSD. We defined the term "resilient" as not having a particular pathology as traditionally defined in the literature (Kaufman, Cook, Arny, Jones, & Pittinsky, 1994). In this study, resilience means not having chronic PTSD secondary to child abuse and neglect so severe that it required Child Protective Services (CPS) involvement. Maltreated youth with chronic PTSD have smaller volumes in the right ventromedial prefrontal cortex (Morey, Haswell, Hooper, & De Bellis, 2016) and posterior cerebral gray matter volumes (De Bellis et al., 2015) compared to maltreated youth without PTSD, demonstrating that structural abnormalities are seen early in the life course of this disease in brain regions associated with executive function, fear extinction, emotion regulation, and memory processing. However, it is not known whether networks as measured by brain structural covariance relationships differ in maltreated youth with versus those resilient to PTSD.

Graph theory provides a framework for characterizing neural networks. A network is defined as a collection of cortical brain regions (nodes) and connections (links paths or edges) between pairs of nodes (Rubinov & Sporns, 2010). Investigators have studied developing brain networks using four approaches (He & Evans, 2010): (a) electrophysiological networks derived from electroencephalogram or magnetoencephalography (van Straaten & Stam, 2012); (b) functional connectivity activations of networks during resting-state functional magnetic resonance imaging (fMRI) or tasks re-

This work has been funded by NIH Grants K24MH71434, K24 DA028773, R01 MH63407, R01 AA12479, and R01 MH61744 (to M.D.D.B.); and VA and NIH Grants VHA VISN 6 MIRECC, VHA CSR&D 5I01CX000120-03, VHA CSR&D 5I01CX000748-03, and NINDS 5R01NS086885-02 (to R.A.M.). This study was presented in poster and abstract form at the American College of Neuropsychopharmacology's 55th Annual Meeting, in Hollywood, Florida, December 4–8, 2016. The authors of this study would like to thank the staff of the Healthy Childhood Brain Development Research Program, and the individuals who participated in this study.

Address correspondence and reprint requests to: Michael D. De Bellis, Department of Psychiatry and Behavioral Sciences, Duke University Medical Center, Box 104360, Durham, NC 27710; E-mail: michael.debellis@duke.edu.

lated deactivations (Fair et al., 2008); (c) structural connectivity networks based on diffusion tensor imaging (DTI) of fiber tracts (Hofer & Frahm, 2006; Raffelt et al., 2017); and (d) structural connectivity networks delineated by between subject intraregional correlations in measures of cortical thickness or gray matter volume (Gong, He, Chen, & Evans, 2012; He & Evans, 2010).

Electrophysiological approaches show increases in average clustering and path length and decreased weight dispersion, indicating that healthy youth brain maturation is characterized by a shift from random to more organized and efficient small-world functional networks (Boersma et al., 2011). Using fMRI, Fair et al. (2008) found that the brain's "default mode network" (DMN), a set of brain regions characterized by decreased neural activity during goal-oriented tasks that are related to internal emotional perception, self-referential thinking, self-awareness, and theory of mind are sparsely functionally connected at early school age (7–9 years) as homotopic regions in the contralateral hemisphere appear to be relatively strong in children; however, children lack the highly integrated strongly functionally connected cortical networks arising from nodes in the posterior cingulate and lateral parietal brain regions (Fair et al., 2008), networks needed for internally directed cognition, regulation of attention, and conscious awareness (Leech & Sharp, 2014). In an examination of the DMN between adults and children using both fMRI and structural maturation DTI, it was observed that white matter structural connectivity between posterior cingulate cortex and left medial temporal lobes was either weak or nonexistent in children, despite the fact that DMN functional connectivity in these brain regions did not differ from adults (Supekar et al., 2010). Because self-monitoring and social cognitive functions mature from childhood to adulthood, the authors concluded that structural connectivity plays an important role in the mature development of self-related and social–cognitive functions that emerge during adolescence.

In this study, we used the structural connectivity network approach based on between-subject intraregional correlations in measures of cortical thickness to examine potential differences in network architecture in maltreated youth with PTSD versus those resilient to PTSD. Cortical morphometric network analysis is an approach based on the observation that cortical thickness or gray matter volumes between two brain regions (e.g., frontal and temporal) correlate across individuals and that this is due to structural relations between these regions that may represent functional associations (Gong et al., 2012). Recently, graph theoretical applications have been used to measure the structural covariance networks of healthy individuals and those with psychiatric disorders (Gong et al., 2012, 2014; He & Evans, 2010; Teicher, Anderson, Ohashi, & Polcari, 2014). Centrality or connectedness is an indicator of the importance of a region within a network of interconnected cortical regions or nodes. Graph theory postulates that cortical regions or nodes with high centrality play an important role in controlling neural communication and network information transfer (He, Chen, & Evans, 2007). As reviewed above, there is a growing appreciation that the brain is organized into complex networks that evolve throughout development, especially in the postnatal and adolescent periods (Di Martino et al., 2014). Network architecture can be inferred from structural covariance derived from between-subject interregional correlations of cortical thickness or gray matter volume. Compared to the functional connectivity networks based on functional imaging data, structural covariance network analysis is less likely to be affected by task requirements and subjects' responses during scanning. Moreover, a recent study by Gong et al. (2012) suggested that cortical thickness correlations reflect unique information representing an important aspect of interregional associations/interactions of the brain network and should not be regarded as a proxy measure for fiber connections measured by DTI (Gong et al., 2012).

Results of cross-sectional imaging studies using a variety of techniques in children and adults who experienced childhood maltreatment compared to nonmaltreated controls suggest that the growth trajectory and remodeling of these networks may be disrupted by maltreatment (Teicher et al., 2016). Although there is one study on structural covariance network in adults who were maltreated as children (Teicher et al., 2014) and one in combat veterans with PTSD (Mueller et al., 2015), there are no published structural covariance network studies in maltreated youth with PTSD. Young adults with maltreatment histories showed altered network centralities compared to adults without maltreatment histories (Teicher et al., 2014), which included lower centrality in the left anterior cingulate gyrus, and increased centrality in right precuneus and right anterior insula in adults with maltreatment histories. The authors' interpretation was that maltreatment is associated with decreased centrality in regions involved in emotion regulation and social cognition, and enhanced centrality in regions involved in internal emotional perception, self-referential thinking, and self-awareness. A brain imaging study using graph analysis restricted to the prefrontal-limbic network showed increased structural connectivity in veterans with PTSD compared to veterans without PTSD. The findings were consistent with greater atrophy and less integration and less global structural connectivity of the prefrontal-limbic network with the rest of the brain in adults with combat-related PTSD that may contribute to the pervasiveness of adult PTSD (Mueller et al., 2015). This study focused on adult onset PTSD, so we do not know how neural networks develop in children with PTSD secondary to experience-unexpected chronic interpersonal traumas like maltreatment.

To address the aforementioned gaps, we examined the brain structural networks of maltreated youth with chronic PTSD and maltreated youth resilient to chronic PTSD. Identifying the brain network characteristics associated with these groups may identify targets for interventions that diminish the enduring effects of maltreatment-related PTSD. Given that maltreated youth with PTSD show developmental differences such as smaller cerebral cortex and cerebellum in pediatric maltreatment-related PTSD (De Bellis & Kuchibhatla, 2006; De Bellis et al., 1999, 2015) and similarities to adult PTSD (de-

https://doi.org/10.1017/S0954579418000093 Published online by Cambridge University Press

creased right ventromedial prefrontal or orbital frontal cortex; Morey et al., 2016), we examined if maltreated youth with PTSD would show similar brain structural covariance network centrality findings to adults with maltreatment history and with combat related PTSD. We hypothesized that maltreated youth with PTSD would show differences of the network centrality of cortical regions or nodes associated with emotional processing, social cognition, and inhibitory control such as the anterior cingulate cortex, posterior cingulate cortex, and inferior frontal cortex/insula compared to maltreated youth without PTSD and nonmaltreated control youth. We also hypothesized that maltreated youth with PTSD would show network centrality differences in nodes in the frontal pole, given that adults with combat-related PTSD have shown relationships between frontopolar cortical thickness and PTSD symptoms (Sadeh et al., 2015, 2016). We were particularly interested in differences that were unique to PTSD (e.g., where centrality was greater than or less than both the maltreated youth without PTSD and control groups) as these differences would suggest psychopathology. We examined differences that were unique to the maltreated group (e.g., where centrality was greater than or less than both the PTSD and control groups) as these differences would suggest resilience to chronic PTSD in youth along with its associated comorbidities. We also planned an examination of differences that were unique to controls (e.g., where centrality was greater than or less than both maltreated groups).

Method

Participants

Detailed demographic, clinical, maltreatment, and PTSD information of subjects are described in Table 1. All participants (57 nonmaltreated healthy youth, 32 maltreated without PTSD and 31 with PTSD) were common to those recruited for our previous study on extinction-related brain structural volumes (Morey et al., 2016) and brain volumes (De Bellis et al., 2015). Briefly, maltreated youth had a positive forensic investigation conducted by CPS that indicated physical and sexual abuse and/or neglect. To examine psychiatric diagnoses, including DSM-IV-TR and DSM-5 for PTSD criteria status and maltreatment characteristics, the Kiddie Schedule for Affective Disorders and Schizophrenia—Present and Lifetime Version (Kaufman et al., 1997) was administered to all caregivers and youth. Because multiple sources of information are needed to gather accurate maltreatment history and related symptoms, we requested and reviewed school, medical, and mental health records (e.g., pediatric records, school attendance records, birth records, and forensics records) as additional data sources of mental health, birth history, trauma history, and pediatric health (Kaufman, Jones, Stieglitz, Vitulano, & Mannarino, 1994). If information from these data sources produced evidence meeting any of the exclusionary criteria, the participant was excluded. Kiddie Schedule for Affective Disorders and Schizophrenia—Present and Lifetime Version interviewer training and modifications have been previously described (De Bellis, Hooper, Spratt, & Woolley, 2009). Healthy nonmaltreated control participants were recruited to be of similar age, gender, handedness, race/ethnicity, and socioeconomic status (SES) to the maltreated groups. IQ was measured by the two-subsets short-form (vocabulary and block design) of the Wechsler Intelligence Scale for Children—III (Wechsler, 1991). Healthy participants' IQ for inclusion was limited to within 1 standard error of measurement (3 IQ points) of the lowest and highest scores of the maltreated youth to control for the inherent confound of lower IQ reported in a well-designed prospective study of individuals with CPS maltreatment histories (Perez & Widom, 1994). After the study was described to the legal guardians

Table 1. *Demographic and clinical information*

	CONT ($N = 57$)	MALT ($N = 32$)	PTSD ($N = 31$)	Statistics	Group differences
Age in years (*SD*)	10.8(2.5)	10.0(2.7)	9.9(2.5)	F (1, 119) = 1.79	*ns*
Age range	6.4–16.1	6.3–16.2	6.2–15.7		
Gender (M/F)	25/32	15/17	15/16	$\chi^2 = 0.18$	*ns*
Handedness (L/R)	6/51	2/30	3/28	$\chi^2 = 0.50$	*ns*
Race (Caus/AA/other)	23/26/8	13/14/5	14/15/2	$\chi^2 = 1.63$	*ns*
SES	41.9(12.9)	38.5(15.8)	37.5(13.8)	F (1, 119) = 1.20	*ns*
IQ	102.2(11.6)	93.0(12.6)	92.6(12.1)	F (1, 119) = 9.27**	CONT > MALT CONT > PTSD
CBCL	40.4(8.8)	57.2(11.7)	64.6(9.7)	F (1, 119) = 68.2***	CONT < MALT MALT < PTSD
CGAS	89.2(5.8)	67.8(9.1)	55.0(7.4)	F (1, 119) = 242.4***	CONT > MALT MALT > PTSD
PTSD symptoms	—	3.57(2.5)	11.51(2.3)	F (1, 62) = 162.1***	MALT < PTSD
Number of Axis I disorders	—	1.00(.98)	3.58(1.61)	F (1, 62) = 59.5***	MALT < PTSD

Note: Numbers of male(M)/female(F), left(L)/right(R) and Caucasian(Cau)/African American(AA)/multiracial(other) are shown for the variables of gender, handedness, and race, respectively. Mean (std) values are displayed for the other variables. **$p < .001$, ***$p < .0001$ for the statistics. The pairwise comparisons employed Tukey's test. CBCL, Child Behavior Checklist total score; CGAS, Children's Global Assessment Scale score; IQ, full-scale IQ estimated from two factors; *ns*, no significant group differences. SES, socioeconomic status measured by the Hollingshead Four-Factor Index. CONT, nonmaltreated controls; MALT, maltreated youth without PTSD; PTSD, maltreated youth with PTSD.

https://doi.org/10.1017/S0954579418000093 Published online by Cambridge University Press

and participants, written informed consent/assents were obtained prior to undertaking this institutional review board-approved study. The PTSD group had chronic PTSD with an age of onset of 6.9 years and age of onset range of age 3–12.5 years with mean PTSD duration of 2.9 years. The PTSD group also had greater Axis I comorbidity than the maltreated without PTSD group. The Child Behavior Checklist was used to measure the total behavior problems reported by the child's caregiver. The Children Global Assessment Scale (Shaffer et al., 1983) was employed to provide a continuous measure of child function by the interviewer after assessing all clinical data. Child Behavior Checklist and Children Global Assessment Scale were reported to give the readers a complete endophenotype of our sample.

Exclusion criteria included IQ <70, chronic medical illness, daily prescription medication, head injury with loss of consciousness, traumatic brain injury, neurological disorder, schizophrenia, anorexia nervosa, pervasive developmental disorder, obsessive–compulsive disorder, bipolar I disorder or mania, birth weight under 5 lbs., or severe prenatal (e.g., fetal alcohol and/or drug exposure) or perinatal (e.g., neonatal intensive care unit stay) complications, current or lifetime nicotine dependence or alcohol/substance use disorder, contraindications for safe MRI scanning, and Axis I disorder or report of maltreatment that warranted CPS investigation in nonmaltreated controls. These criteria minimize the influences of prenatal substance exposure, low SES, alcohol and substance dependence, use of psychotropic medications, and medical illnesses that are overrepresented in maltreated youth and can independently negatively influence brain maturation (Hussey, Chang, & Kotch, 2006; Leslie et al., 2005; Raghavan et al., 2005; Smith, Johnson, Pears, Fisher, & DeGarmo, 2007).

MRI acquisition

We acquired high-resolution T1-weighted magnetic resonance images using the same Siemens Trio 3.0 Tesla MRI system (Trio, Siemens Medical Systems) scanner (3D, GRE [MPRAGE], axial, resonance time/echo time/flip angle/field of view/slice thickness = 1750 ms/1100 ms/20°/256 mm/1.0 mm, bandwidth [220 Hz/pixel] = 256 [phase] × 256 [frequency], number of excitations = 1). We visually inspected all T1 images to assure high quality, and employed a neuroradiologist to review images to rule out clinically significant abnormalities. Youth with brain scans with clinically significant abnormalities were excluded, and these subjects' data were not reported in this study.

Network analyses

Cortical morphometric networks were determined using previously published procedures of structural covariance analyses (Gong et al., 2012; Teicher et al., 2014). First, cortical reconstruction and thickness analyses using automated segmentation and labeling with the FreeSurfer image analysis suite (version 5.1.0; http://surfer.nmr.mgh.harvard.edu/) and its library tool recon-all were implemented by applying the standardized procedures (Morey et al., 2016). Second, we calculated the cortical thickness for 148 cortical regions (nodes) using the aparc.a2009s template (Destrieux, Fischl, Dale, & Halgren, 2010). We undertook structural covariance analyses using previously published methods (Gong et al., 2012; Teicher et al., 2014), implemented with internally developed Matlab (ver. 2016a) scripts running on an Apple iMac-27 computer (OS Sierra version 10.12.6). We then generated interregional partial correlation matrices for each group by calculating partial correlation coefficient for all regional pairings of cortical thickness measures across subjects within each of the three groups (He et al., 2009; Mueller et al., 2015). The partial correlation between any two cortical regions represented their conditional dependencies after regressing out the effects of covariates, including gender, age, handedness, and SES, because these factors are associated with brain structural volume changes in this developmental stage (Morey et al., 2016). Then, we thresholded the matrices to create a binary graph that represented strong (suprathreshold) partial correlations as connections (edges) between cortical regions. The threshold was group specific so that the graphs of all groups had the same number of connections or wiring cost (number of edges divided by maximum possible number of edges). Here, we were interested in the between-group differences of network configurations (with the same number of connections) but not the number of paths. To obtain the group-specific threshold, we calculated the minimum wiring cost (0.3074 for controls; 0.2583 for maltreated without PTSD, and 0.1218 for maltreated with PTSD) required to produce fully connected networks for each group, and then selected the largest wiring cost across groups and calculated the corresponding threshold for each group. This method ensured that all nodes were included in the network while minimizing the number of redundant paths. That is to say, the network of controls (the group with the largest wiring cost) was fully connected without redundant paths, while the networks of maltreated youth with or without PTSD were also fully connected but demonstrated a few redundant connections (while the redundancy was limited by the maximal wiring cost). We only investigated positive suprathreshold partial correlations in the networks due to a previous report that positive but not negative thickness covariance may reflect long-range structural connections (Gong et al., 2012).

Centrality measures

Following previously described methods in adult studies of maltreatment and PTSD (Mueller et al., 2015; Teicher et al., 2014), we investigated four types of centrality measures using the Brain Connectivity Toolbox (Rubinov & Sporns, 2010). The centrality measures were degree centrality (number of directly interconnected nodes), betweenness centrality (frequency with which a node falls between pairs of other nodes on their shortest interconnecting path), closeness centrality (normalized number of steps required to access every

https://doi.org/10.1017/S0954579418000093 Published online by Cambridge University Press

other node from a given node in a network, adapted from the distance function in the Brain Connectivity Toolbox), and eigenvector centrality (a spectral centrality measure based on the idea that the importance of a node is related to the importance of the nodes connected with it).

Examination of between-groups centrality statistical analyses

We excluded from further analyses the cortical regions showing unequal variances (see Table 2) for the between-group comparisons on centralities (two-sample F tests at the 1% significance level), given that the variances in the groups' measures should be equal despite the different sample sizes (Winkler, Webster, Vidaurre, Nichols, & Smith, 2015). We then calculated and found that all centralities were within their 99% confidence interval through the Jackknife resampling method (Efron & Tibshirani, 1993), supporting the reliability of the centrality measures. After that, and as a methodological improvement to previous brain structural covariance network studies, we employed principle component analysis (PCA) methods to convert the four centrality measures into four linearly uncorrelated components, in which the first two components explained more than 98% of the variance contained in the four centrality measures (Table 3). Our following analyses were based on the first two PCA components. PCA was used here to reduce redundant information because the four centralities were highly correlated to each other (Pearson correlation coefficients $>$ .59, $ps < .001$) and thus may reflect similar graph characteristics. The previous study by Teicher et al. (2014) reported findings that were significant in at least two of four between-group comparisons of centrality. However, it is now thought that their method may inflate either false positive or false negative results. For example, degree, closeness, and eigenvector centralities may reflect overlapping information, and weak group differences shared by these measures is likely to be reported as a significant between-group difference. For another instance, betweenness centrality may reflect information different from other centralities, and even very significant between-group differences in betweenness will not be reported because there are no accompanying group differences in the other centralities. Here, the PCA method contributes to (a) transforming the centralities into components orthogonal to each other, and (b) reducing the number of variables during statistical corrections for multiple comparisons. Examination of two PCA components showed that the first PCA component was mainly explained by degree and eigenvector centralities (principle component coefficients: 0.52 $\sim$ 0.63), and then by the betweenness and closeness degrees (principle component coefficients: 0.29 $\sim$ 0.46). The second PCA component was mainly explained by the betweenness centrality (principle component coefficient: 0.88 $\sim$ 0.92). Finally, we performed between-group comparisons on the two PCA components with permutation testing to calculate the probability that the differences could have occurred by chance based on 10,000 network comparisons derived by randomly assigning subjects to two groups (He, Chen, & Evans, 2008; Zalesky, Fornito, & Bullmore, 2010). We applied the Bonferroni method to correct for the multiple comparisons across three between-group contrasts and two PCA components, that is $p < .05 / (3 \times 2) = .008$. We also corrected for the number of nodes ($N = 148$) in regions of no interest by using the Bonferroni method, $p < .05 / (3 \times 2 \times 148) = 6.0 \times 10^{-5}$.

Table 2. *Cortical areas showing unequal variances for the between-group comparisons on centralities*

	Cortical area label	
Comparison	Left hemisphere	Right hemisphere
MALT vs. CONT	63	25, 26, 34, 38
PTSD vs. CONT	11, 25, 42, 57, 67	11, 27, 42
PTSD vs. MALT	25, 27, 42, 67	15, 19, 26, 42

Note: The areas listed here were excluded from further analyses in the corresponding between-group contrast. Cortical area labels were according to Destrieux et al. (2010). CONT, nonmaltreated controls; MALT, maltreated youth without PTSD; PTSD, maltreated youth with PTSD.

Table 3. *Variance of centralities explained by PCA components*

	PCA component			
Group	1	2	3	4
CONT	88.80%	9.90%	1.20%	0.10%
MALT	91.60%	7.90%	0.40%	0.10%
PTSD	89.40%	9.60%	0.80%	0.20%

Note: CONT, nonmaltreated controls; MALT, maltreated youth without PTSD; PTSD, maltreated youth with PTSD.

Examination of between-groups cortical thickness statistical analyses

We also investigated the between-group differences of cortical thickness through using independent t tests. We applied Bonferroni methods to correct for the multiple comparisons across three between-group contrasts, that is, $p < .05 / 3 = .016$. We also corrected for the number of nodes ($N = 148$) in regions of no interest by using the Bonferroni method, $p < .05 / (3 \times 148) = 1.0 \times 10^{-4}$.

Results

Centrality measures

Significant between-group differences ($p < .05$; corrected) based on the first two PCA components are summarized in Table 4 and Figure 1. The original centrality values are also

https://doi.org/10.1017/S0954579418000093 Published online by Cambridge University Press

Table 4. *Cortical areas showing significant between-group differences in any of the first two PCA components for the four centralities*

No.	ROI	Cortical areas	Group differences	Centralities (CONT/MALT/PTSD)
			Left hemisphere	
7	ACC	Middle-anterior part of the cingulate gyrus and sulcus[2]	MALT > PTSD	Deg: 56/57/55 Bet: 95.6/336.9/57.2 Clo: 0.680/0.689/0.672 Eig: 0.093/0.078/0.104
71	PCC	Subparietal sulcus[2]	CONT > MALT CONT > PTSD	Deg: 33/64/66 Bet: 308.2/113.9/159.0 Clo: 0.598/0.712/0.724 Eig: 0.051/0.107/0.121
			Right hemisphere	
5	FP	Transverse frontopolar gyri and sulci[2]	MALT > CONT MALT > PTSD	Deg: 41/54/35 Bet: 39.9/350.0/86.9 Clo: 0.629/0.679/0.609 Eig: 0.068/0.090/0.033
9	PCC	Posterior-dorsal part of the cingulate gyrus[1]	MALT < PTSD	Deg: 26/8/65 Bet: 20.5/0.8/230.0 Clo: 0.575/0.485/0.720 Eig: 0.041/0.007/0.118
13	IFC	Orbital part of the inferior frontal gyrus[1]	MALT > PTSD	Deg: 47/62/12 Bet: 211.9/320.7/40.7 Clo: 0.654/0.711/0.524 Eig: 0.073/0.087/0.011
14	IFC	Triangular part of the inferior frontal gyrus[1]	MALT > PTSD	Deg: 73/88/24 Bet: 362.2/359.4/21.4 Clo: 0.742/0.798/0.580 Eig: 0.114/0.135/0.039
46	PCC	Marginal branch (or part) of the cingulate sulcus[1]	CONT < PTSD	Deg: 60/76/85 Bet: 98.5/274.8/343.9 Clo: 0.694/0.756/0.789 Eig: 0.099/0.124/0.146
52	IFC	Inferior frontal sulcus[2]	CONT > MALT CONT > PTSD	Deg: 30/69/46 Bet: 266.1/152.6/104.1 Clo: 0.588/0.734/0.655 Eig: 0.049/0.112/0.082

Note: [1,2], Significant differences were detected in the first and second PCA components, respectively. Results survived Bonferroni correction for the multiple comparisons across three between-group comparisons as well as the first two PCA components, that is, $p < .05 / (3 \times 2) = .008$. Numbers and names of the cortical areas were according to Destrieux et al. (2010). ROI, cortical regions of interest include anterior cingulate cortex (ACC), frontal pole (FP), inferior frontal cortex (IFC), and posterior cingulate cortex (PCC). Values of four centralities (Deg, degree centrality; Bet, betweenness centrality; Clo, closeness centrality; and Eig, eigenvector centrality) were also listed for reference. CONT, nonmaltreated controls; MALT, maltreated youth without PTSD; PTSD, maltreated youth with PTSD.

listed in Table 4 to clarify the topological meaning. For our research aims, we specifically investigated the differences unique to one group compared to the other two groups in these nodes: the anterior cingulate cortex (ACC), the posterior cingulate cortex (PCC), the inferior frontal cortex/insula (IFC), and the frontal pole (FP).

Maltreated youth with PTSD compared to the other two groups showed larger values of PCA components in the right PCC and smaller PCA values in the right IFC. More specifically, maltreated youth with PTSD versus without PTSD exhibited a larger centrality value in PCA Component 1 in only one node, the right posterior-dorsal part of the cingulate gyrus (PCC, area 9, according to Destrieux et al., 2010). Maltreated youth with PTSD versus those resilient to PTSD demonstrated smaller centrality values in Component 1 in the right orbital part of the IFC (area 13) and the right triangular part of the inferior frontal gyrus (IFC, area 14). Moreover, maltreated youth with PTSD versus nonmaltreated controls showed a greater centrality measure in Component 1 in the right marginal branch (or part) of the cingulate sulcus (PCC, area 46), and a smaller centrality measure in Component 2 in the right inferior frontal sulcus (IFC, area 52).

In addition, we also found that maltreated youth with versus resilient to PTSD showed a smaller value in Component 2 in the left middle-anterior part of the cingulate gyrus and sulcus (ACC, area 7). No other between-group difference was found significant in ACC.

Maltreated youth resilient to PTSD compared to the other two groups showed larger centrality values in Component 2 in the right transverse frontopolar gyri and sulci (FP, area 5).

https://doi.org/10.1017/S0954579418000093 Published online by Cambridge University Press

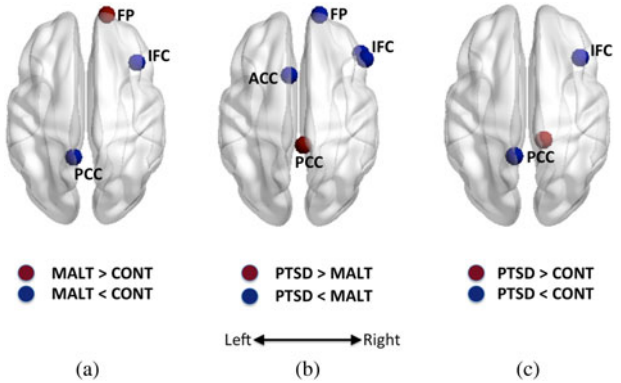

Figure 1. (Color Online) Nodes showing significant between-group difference in any of the first two components for the four nodal centralities. Pairwise comparisons among maltreated youth without posttraumatic stress disorder (PTSD; MALT group), with PTSD (PTSD group), and nonmaltreated controls (CONT group) were exhibited in subpanels A, B, and C. Results survived corrections ($p < .05$). ACC, anterior cingulate cortex (area 7); FP, frontal pole (area 5); IFC, inferior frontal cortex (areas 13, 14, and 52); PCC, posterior cingulate cortex (areas 9, 46, and 71). The labels of cortical areas were according to Destrieux et al. (2010).

These findings indicate cortical brain nodes uniquely affected by resilience to maltreatment-related PTSD.

Nonmaltreated controls compared to the other two groups exhibited larger values in Component 2 in the left subparietal sulcus (PCC, area 71) and the right inferior frontal sulcus (IFC, area 52). These findings indicate cortical brain nodes uniquely affected by maltreatment.

Cortical thickness

No results survived correction for multiple comparisons. Mean values, standard deviations, and between-group *t* test results (uncorrected) are listed in Table 5.

Discussion

To the best of our knowledge, this is the first investigation comparing structural covariance networks defined by cortical thickness in maltreated youth with and those resilient to chronic PTSD. Consistent with our a priori hypothesis, we detected significant between-group differences of nodal centralities in the ACC, PCC, IFC, and FP that were unique to (a) pediatric maltreatment-related PTSD (specific to maltreated youth with PTSD compared with two other groups), (b) experiencing maltreatment (specific to both maltreated groups compared to controls), and (c) resilience to chronic PTSD (specific to maltreated youth without PTSD compared to the other two groups).

We did not find any difference in cortical thickness, demonstrating that childhood maltreatment and PTSD are more associated with alterations in interregional relationships of cortical thickness than associated with cortical thickness itself. The cortical thickness finding is opposite to the results of a recent study of adolescents and young adults who experienced physical and sexual abuse compared to nonabused adolescents, which showed reduced cortical thickness in the ventromedial prefrontal cortex, right lateral orbitofrontal cortex, right inferior frontal gyrus, bilateral parahippocampal gyrus, left temporal pole, and bilateral inferior, right middle, and right superior temporal gyri (Gold et al., 2016). However, the mean age of participants in the study by Gold et al. (2016) was 16.97 years (age range 13 to 20 years), while it was 10.4 years (age range 6 to 16 years) in our study. Cortical thickness shows greater decreases with age during adolescence and young adulthood, while increases are seen in the age range of this study (Pfefferbaum et al., 2015). Thus the influences of neurodevelopment may explain the differences in these two studies.

Maltreated youth with PTSD showed larger centrality in the right PCC than the other two groups. Teicher et al. (2014) reported larger centrality in the right precuneus (a brain region physically close to the PCC) in young adults exposed to childhood maltreatment compared to controls. However, it is unknown whether their findings would be attributed to PTSD. The PCC is a key node in the posterior DMN and is related with internally directed cognition, attention regulation, and conscious awareness (Leech & Sharp, 2014). The larger centrality in the right PCC may be accompanied by abnormal functions of self-referential network processing in maltreated youth with PTSD. This thought is in line with the knowledge that intrusive reexperiencing is one of the core symptoms of PTSD and is represented by intrusive images, flashbacks, nightmares, distress, and physiological reactions to reminders of trauma. The maltreated children with PTSD versus those without PTSD may think more frequently about their trauma, the impact of their trauma on their lives, and ruminate more on these themes; these thoughts may be related to the PTSD symptom of intrusive reexperiencing and lead to the lower level of global function we saw in the maltreated youth with chronic PTSD. In support of this idea, increased blood flow in the PCC was reported in women with PTSD compared to those without PTSD when listening to traumatic scripts of personalized childhood sexual abuse events (Bremner et al., 1999). More negative functional connections between the PCC and the bilateral amygdala were also found to relate with more severe PTSD symptoms (Zhou et al., 2012). Previous studies have shown that DMN decreases in connectivity during tasks and increases during rest (Fox et al., 2005), while recent studies showed that the precuneus simultaneously interacts with both DMN and the frontoparietal networks to distinguish different cognitive states (Utevsky, Smith, & Huettel, 2014). Here we found that the PCC plays different roles between groups in the brain network based on structural images. It is possible that the PCC also works differently in maltreated youth with PTSD than the other groups in the brain networks derived from functional imaging studies during both resting state and task engagement. This idea needs to be tested in future studies. Such differences may be associated with symptoms accompanied by childhood maltreatment and/or pediatric PTSD. This study also highlighted the crucial role of the

https://doi.org/10.1017/S0954579418000093 Published online by Cambridge University Press

Table 5. *Cortical thickness of three groups*

No.	Area	CONT	MALT	PTSD	MALT vs. CONT	PTSD vs. CONT	PTSD vs. MALT
		mean(*SD*)			*t*(*p*)		
1	L Fronto-marginal gyrus (of Wernicke) and sulcus	2.54(0.25)	2.56(0.29)	2.57(0.23)	0.432(.667)	0.624(.534)	0.124(.902)
2	L Inferior occipital gyrus and sulcus	2.35(0.17)	2.41(0.24)	2.47(0.17)	1.464(.147)	3.481(.001)	1.275(.207)
3	L Paracentral lobule and sulcus	2.43(0.17)	2.42(0.18)	2.41(0.23)	−0.236(.814)	−0.466(.643)	−0.206(.837)
4	L Subcentral gyrus (central operculum) and sulci	2.76(0.23)	2.76(0.20)	2.79(0.20)	−0.045(.964)	0.647(.519)	0.675(.502)
5	L Transverse frontopolar gyri and sulci	2.87(0.30)	2.91(0.32)	2.83(0.33)	0.713(.478)	−0.441(.661)	−0.967(.337)
6	L Anterior part of the cingulate gyrus and sulcus	2.91(0.21)	2.98(0.22)	2.92(0.26)	1.362(.177)	0.200(.842)	−0.900(.372)
7	L Middle-anterior part of the cingulate gyrus and sulcus	2.84(0.19)	2.79(0.19)	2.86(0.25)	−1.184(.240)	0.293(.770)	1.139(.259)
8	L Middle-posterior part of the cingulate gyrus and sulcus	2.82(0.18)	2.85(0.20)	2.83(0.14)	0.788(.433)	0.488(.627)	−0.349(.728)
9	L Posterior-dorsal part of the cingulate gyrus	3.22(0.23)	3.27(0.21)	3.17(0.25)	1.012(.314)	−0.911(.365)	−1.674(.099)
10	L Posterior-ventral part of the cingulate gyrus	2.36(0.29)	2.42(0.25)	2.40(0.27)	0.971(.334)	0.638(.525)	−0.302(.764)
11	L Cuneus	1.85(0.16)	1.90(0.15)	1.98(0.32)	1.445(.152)	2.695(.008)	1.356(.180)
12	L Opercular part of the inferior frontal gyrus	2.98(0.18)	2.96(0.19)	2.94(0.22)	−0.515(.608)	−0.972(.334)	−0.390(.698)
13	L Orbital part of the inferior frontal gyrus	3.06(0.33)	3.24(0.31)	3.10(0.38)	2.487(.015)	0.432(.667)	−1.644(.105)
14	L Triangular part of the inferior frontal gyrus	2.97(0.26)	2.96(0.29)	2.98(0.25)	−0.183(.855)	0.309(.758)	0.417(.678)
15	L Middle frontal gyrus	2.90(0.22)	2.92(0.19)	2.92(0.18)	0.569(.571)	0.431(.667)	−0.146(.885)
16	L Superior frontal gyrus	3.06(0.22)	3.05(0.18)	3.03(0.26)	−0.213(.832)	−0.491(.625)	−0.275(.784)
17	L Long insular gyrus and central sulcus of the insula	3.01(0.33)	3.00(0.35)	2.92(0.32)	−0.189(.851)	−1.324(.189)	−0.957(.342)
18	L Short insular gyri	3.33(0.26)	3.37(0.29)	3.26(0.33)	0.578(.565)	−1.109(.270)	−1.331(.188)
19	L Middle occipital gyrus	2.66(0.25)	2.65(0.26)	2.69(0.24)	−0.303(.763)	0.561(.576)	0.763(.449)
20	L Superior occipital gyrus	2.25(0.17)	2.29(0.18)	2.34(0.24)	0.923(.358)	1.960(.053)	0.932(.355)
21	L Lateral occipito-temporal gyrus (fusiform gyrus)	2.81(0.20)	2.86(0.25)	2.88(0.21)	1.045(.299)	1.514(.134)	0.297(.767)
22	L Lingual gyrus	1.98(0.17)	2.03(0.18)	2.10(0.24)	1.283(.203)	2.735(.008)	1.292(.201)
23	L Parahippocampal gyrus	2.70(0.24)	2.77(0.26)	2.73(0.23)	1.179(.242)	0.624(.534)	−0.525(.602)
24	L Orbital gyri	2.80(0.22)	2.85(0.22)	2.80(0.24)	0.982(.329)	−0.010(.992)	−0.828(.411)
25	L Angular gyrus	3.01(0.28)	3.00(0.29)	3.04(0.18)	−0.106(.916)	0.511(.610)	0.580(.564)
26	L Supramarginal gyrus	2.98(0.26)	2.95(0.23)	2.94(0.17)	−0.596(.553)	−0.894(.374)	−0.246(.807)
27	L Superior parietal lobule	2.62(0.21)	2.60(0.19)	2.64(0.29)	−0.455(.650)	0.482(.631)	0.739(.463)
28	L Postcentral gyrus	2.28(0.20)	2.26(0.19)	2.23(0.18)	−0.554(.581)	−1.183(.240)	−0.544(.588)
29	L Precentral gyrus	2.84(0.20)	2.81(0.20)	2.78(0.24)	−0.739(.462)	−1.311(.193)	−0.534(.595)
30	L Precuneus	2.81(0.20)	2.85(0.22)	2.81(0.17)	0.698(.487)	−0.017(.987)	−0.684(.497)
31	L Straight gyrus, Gyrus rectus	2.62(0.23)	2.63(0.26)	2.60(0.25)	0.163(.871)	−0.415(.679)	−0.481(.632)
32	L Subcallosal area	2.13(0.30)	2.15(0.26)	2.19(0.34)	0.366(.715)	0.891(.375)	0.508(.613)
33	L Anterior transverse temporal gyrus (of Heschl)	2.30(0.25)	2.36(0.30)	2.31(0.28)	1.003(.319)	0.055(.956)	−0.781(.438)
34	L Lateral aspect of the superior temporal gyrus	2.91(0.22)	2.91(0.25)	2.88(0.26)	0.079(.937)	−0.532(.596)	−0.495(.622)
35	L Planum polare of the superior temporal gyrus	2.57(0.36)	2.69(0.35)	2.64(0.50)	1.509(.135)	0.848(.399)	−0.392(.697)
36	L Planum temporale or temporal plane of the superior temporal gyrus	2.78(0.20)	2.76(0.22)	2.72(0.24)	−0.392(.696)	−1.203(.232)	−0.661(.511)
37	L Inferior temporal gyrus	2.77(0.22)	2.85(0.20)	2.81(0.23)	1.661(.100)	0.656(.513)	−0.849(.399)
38	L Middle temporal gyrus	3.07(0.21)	3.09(0.23)	3.07(0.19)	0.424(.673)	−0.025(.980)	−0.410(.683)
39	L Horizontal ramus of the anterior segment of the lateral sulcus	2.52(0.34)	2.68(0.31)	2.59(0.35)	2.181(.032)	0.914(.363)	−1.092(.279)
40	L Vertical ramus of the anterior segment of the lateral sulcus	2.68(0.25)	2.63(0.25)	2.62(0.34)	−0.940(.350)	−0.968(.335)	−0.107(.915)
41	L Posterior ramus (or segment) of the lateral sulcus	2.58(0.20)	2.55(0.19)	2.56(0.22)	−0.696(.488)	−0.463(.645)	0.178(.859)

https://doi.org/10.1017/S0954579418000093 Published online by Cambridge University Press

Table 5 (*cont.*)

No.	Area	CONT	MALT	PTSD	MALT vs. CONT	PTSD vs. CONT	PTSD vs. MALT
		mean(*SD*)			*t*(*p*)		
42	L Occipital pole	1.87(0.14)	1.89(0.20)	2.06(0.33)	0.580(.563)	3.740(.000)	2.394(.020)
43	L Temporal pole	2.42(0.31)	2.58(0.38)	2.40(0.31)	2.170(.033)	−0.313(.755)	−2.118(.038)
44	L Calcarine sulcus	1.98(0.12)	2.01(0.16)	2.08(0.17)	0.953(.343)	3.145(.002)	1.652(.104)
45	L Central sulcus	1.97(0.11)	1.92(0.12)	1.95(0.15)	−2.118(.037)	−0.833(.407)	0.900(.371)
46	L Marginal branch (or part) of the cingulate sulcus	2.49(0.20)	2.50(0.22)	2.49(0.19)	0.217(.829)	0.010(.992)	−0.187(.853)
47	L Anterior segment of the circular sulcus of the insula	2.91(0.26)	2.94(0.32)	2.84(0.36)	0.432(.667)	−1.092(.278)	−1.171(.246)
48	L Inferior segment of the circular sulcus of the insula	2.76(0.22)	2.74(0.22)	2.77(0.20)	−0.421(.675)	0.288(.774)	0.646(.521)
49	L Superior segment of the circular sulcus of the insula	2.74(0.18)	2.75(0.19)	2.74(0.22)	0.290(.772)	−0.005(.996)	−0.234(.816)
50	L Anterior transverse collateral sulcus	2.64(0.32)	2.64(0.25)	2.56(0.28)	0.089(.929)	−1.167(.246)	−1.248(.217)
51	L Posterior transverse collateral sulcus	2.11(0.22)	2.18(0.26)	2.25(0.27)	1.235(.220)	2.542(.013)	1.051(.297)
52	L Inferior frontal sulcus	2.50(0.15)	2.49(0.20)	2.48(0.18)	−0.433(.666)	−0.582(.562)	−0.092(.927)
53	L Middle frontal sulcus	2.43(0.19)	2.42(0.20)	2.49(0.28)	−0.322(.748)	1.205(.231)	1.217(.228)
54	L Superior frontal sulcus	2.50(0.21)	2.47(0.19)	2.51(0.23)	−0.672(.504)	0.129(.897)	0.686(.495)
55	L Sulcus intermedius primus (of Jensen)	2.65(0.51)	2.67(0.44)	2.56(0.46)	0.148(.883)	−0.829(.410)	−0.933(.355)
56	L Intraparietal sulcus (interparietal sulcus) and transverse parietal sulci	2.34(0.17)	2.31(0.18)	2.39(0.17)	−1.007(.317)	1.333(.186)	1.997(.050)
57	L Middle occipital sulcus and lunatus sulcus	2.13(0.17)	2.13(0.18)	2.21(0.27)	0.106(.916)	1.746(.084)	1.343(.184)
58	L Superior occipital sulcus and transverse occipital sulcus	2.25(0.18)	2.28(0.22)	2.33(0.20)	0.702(.485)	2.154(.034)	1.107(.272)
59	L Anterior occipital sulcus and preoccipital notch	2.39(0.18)	2.40(0.26)	2.40(0.22)	0.169(.867)	0.352(.726)	0.120(.905)
60	L Lateral occipito-temporal sulcus	2.60(0.21)	2.66(0.24)	2.61(0.20)	1.244(.217)	0.391(.697)	−0.797(.428)
61	L Medial occipito-temporal sulcus (collateral sulcus) and lingual sulcus	2.49(0.18)	2.47(0.22)	2.52(0.20)	−0.429(.669)	0.638(.525)	0.860(.393)
62	L Lateral orbital sulcus	2.45(0.31)	2.48(0.33)	2.61(0.34)	0.468(.641)	2.321(.023)	1.565(.123)
63	L Medial orbital sulcus	2.30(0.27)	2.34(0.15)	2.29(0.25)	0.686(.495)	−0.200(.842)	−0.926(.358)
64	L Orbital sulci (H-shaped sulci)	2.77(0.29)	2.85(0.27)	2.80(0.27)	1.216(.227)	0.442(.660)	−0.726(.470)
65	L Parieto-occipital sulcus (or fissure)	2.38(0.19)	2.36(0.20)	2.42(0.19)	−0.606(.546)	0.971(.334)	1.339(.185)
66	L Pericallosal sulcus	2.20(0.29)	2.22(0.33)	2.21(0.32)	0.337(.737)	0.206(.837)	−0.114(.910)
67	L Postcentral sulcus	2.36(0.19)	2.32(0.19)	2.33(0.11)	−0.855(.395)	−0.682(.497)	0.284(.777)
68	L Inferior part of the precentral sulcus	2.63(0.17)	2.60(0.19)	2.58(0.23)	−0.693(.490)	−1.101(.274)	−0.356(.723)
69	L Superior part of the precentral sulcus	2.41(0.21)	2.38(0.16)	2.38(0.20)	−0.738(.462)	−0.590(.556)	0.110(.913)
70	L Suborbital sulcus	2.80(0.33)	2.91(0.44)	2.84(0.41)	1.378(.172)	0.487(.628)	−0.712(.479)
71	L Subparietal sulcus	2.60(0.23)	2.63(0.21)	2.63(0.19)	0.657(.513)	0.750(.455)	0.063(.950)
72	L Inferior temporal sulcus	2.58(0.21)	2.68(0.23)	2.56(0.25)	2.033(.045)	−0.548(.585)	−2.094(.040)
73	L Superior temporal sulcus	2.70(0.17)	2.71(0.17)	2.68(0.19)	0.110(.913)	−0.640(.524)	−0.639(.526)
74	L Transverse temporal sulcus	2.62(0.31)	2.60(0.35)	2.59(0.36)	−0.271(.787)	−0.406(.686)	−0.109(.913)
1	R Fronto-marginal gyrus (of Wernicke) and sulcus	2.52(0.25)	2.54(0.34)	2.58(0.23)	0.282(.778)	0.954(.343)	0.457(.649)
2	R Inferior occipital gyrus and sulcus	2.56(0.25)	2.57(0.24)	2.61(0.20)	0.168(.867)	0.915(.363)	0.698(.488)
3	R Paracentral lobule and sulcus	2.37(0.18)	2.38(0.16)	2.39(0.17)	0.207(.836)	0.501(.617)	0.280(.781)
4	R Subcentral gyrus (central operculum) and sulci	2.82(0.23)	2.76(0.21)	2.70(0.15)	−1.082(.282)	−2.431(.017)	−1.239(.220)
5	R Transverse frontopolar gyri and sulci	2.77(0.28)	2.81(0.33)	2.90(0.29)	0.598(.551)	2.136(.035)	1.198(.235)
6	R Anterior part of the cingulate gyrus and sulcus	2.83(0.21)	2.83(0.21)	2.83(0.16)	0.167(.868)	0.121(.904)	−0.055(.956)
7	R Middle-anterior part of the cingulate gyrus and sulcus	2.88(0.20)	2.84(0.24)	2.88(0.18)	−0.756(.452)	0.140(.889)	0.795(.430)
8	R Middle-posterior part of the cingulate gyrus and sulcus	2.82(0.17)	2.81(0.16)	2.76(0.14)	−0.242(.810)	−1.638(.105)	−1.302(.198)
9	R Posterior-dorsal part of the cingulate gyrus	3.16(0.22)	3.24(0.23)	3.13(0.33)	1.740(.085)	−0.443(.659)	−1.556(.125)
10	R Posterior-ventral part of the cingulate gyrus	2.69(0.34)	2.87(0.37)	2.73(0.30)	2.306(.024)	0.642(.523)	−1.561(.124)

https://doi.org/10.1017/S0954579418000093 Published online by Cambridge University Press

Table 5 (*cont.*)

No.	Area	CONT	MALT	PTSD	MALT vs. CONT	PTSD vs. CONT	PTSD vs. MALT
		mean(*SD*)			*t*(*p*)		
11	R Cuneus	1.86(0.15)	1.89(0.17)	1.99(0.27)	0.895(.373)	3.069(.003)	1.824(.073)
12	R Opercular part of the inferior frontal gyrus	3.01(0.19)	2.94(0.22)	2.90(0.25)	−1.546(.126)	−2.399(.019)	−0.728(.469)
13	R Orbital part of the inferior frontal gyrus	3.08(0.36)	3.13(0.35)	3.12(0.39)	0.618(.538)	0.424(.673)	−0.153(.879)
14	R Triangular part of the inferior frontal gyrus	3.02(0.23)	3.03(0.26)	3.02(0.21)	0.315(.753)	−0.014(.989)	−0.294(.770)
15	R Middle frontal gyrus	2.89(0.20)	2.85(0.23)	2.90(0.14)	−0.716(.476)	0.426(.671)	1.057(.295)
16	R Superior frontal gyrus	2.99(0.20)	2.95(0.19)	2.96(0.24)	−1.027(.307)	−0.611(.543)	0.299(.766)
17	R Long insular gyrus and central sulcus of the insula	3.05(0.33)	3.04(0.36)	2.97(0.31)	−0.141(.888)	−1.139(.258)	−0.828(.411)
18	R Short insular gyri	3.42(0.27)	3.39(0.27)	3.25(0.32)	−0.614(.541)	−2.761(.007)	−1.840(.071)
19	R Middle occipital gyrus	2.67(0.24)	2.65(0.35)	2.72(0.21)	−0.316(.753)	0.944(.348)	0.932(.355)
20	R Superior occipital gyrus	2.27(0.20)	2.32(0.21)	2.33(0.24)	1.091(.278)	1.195(.235)	0.131(.896)
21	R Lateral occipito-temporal gyrus (fusiform gyrus)	2.82(0.25)	2.86(0.20)	2.84(0.20)	0.771(.443)	0.411(.682)	−0.371(.712)
22	R Lingual gyrus	2.01(0.19)	2.06(0.14)	2.13(0.25)	1.116(.267)	2.355(.021)	1.326(.190)
23	R Parahippocampal gyrus	2.65(0.24)	2.62(0.25)	2.65(0.25)	−0.645(.521)	−0.155(.877)	0.426(.672)
24	R Orbital gyri	2.85(0.22)	2.82(0.23)	2.81(0.21)	−0.547(.586)	−0.838(.404)	−0.222(.825)
25	R Angular gyrus	3.04(0.24)	2.94(0.38)	2.95(0.33)	−1.428(.157)	−1.371(.174)	0.124(.901)
26	R Supramarginal gyrus	2.97(0.19)	2.87(0.31)	2.91(0.17)	−1.904(.060)	−1.414(.161)	0.713(.478)
27	R Superior parietal lobule	2.59(0.18)	2.54(0.25)	2.53(0.29)	−1.103(.273)	−1.240(.218)	−0.163(.871)
28	R Postcentral gyrus	2.29(0.24)	2.25(0.18)	2.29(0.27)	−0.745(.459)	0.055(.956)	0.678(.500)
29	R Precentral gyrus	2.81(0.23)	2.78(0.23)	2.73(0.29)	−0.704(.483)	−1.502(.137)	−0.715(.477)
30	R Precuneus	2.81(0.25)	2.83(0.28)	2.78(0.20)	0.301(.764)	−0.580(.564)	−0.780(.438)
31	R Straight gyrus, Gyrus rectus	2.49(0.23)	2.53(0.24)	2.53(0.26)	0.731(.467)	0.853(.396)	0.113(.910)
32	R Subcallosal area	2.16(0.33)	2.20(0.29)	2.22(0.41)	0.472(.638)	0.783(.436)	0.322(.749)
33	R Anterior transverse temporal gyrus (of Heschl)	2.37(0.24)	2.30(0.29)	2.42(0.29)	−1.052(.296)	0.920(.360)	1.568(.122)
34	R Lateral aspect of the superior temporal gyrus	2.93(0.19)	2.86(0.30)	2.92(0.22)	−1.430(.156)	−0.365(.716)	0.871(.387)
35	R Planum polare of the superior temporal gyrus	2.58(0.35)	2.53(0.34)	2.54(0.36)	−0.572(.569)	−0.506(.614)	0.057(.954)
36	R Planum temporale or temporal plane of the superior temporal gyrus	2.76(0.17)	2.67(0.23)	2.78(0.24)	−2.016(.047)	0.624(.535)	1.936(.058)
37	R Inferior temporal gyrus	2.82(0.21)	2.82(0.22)	2.82(0.22)	0.169(.866)	0.188(.851)	0.016(.987)
38	R Middle temporal gyrus	3.10(0.18)	3.11(0.27)	3.12(0.23)	0.289(.773)	0.612(.542)	0.205(.838)
39	R Horizontal ramus of the anterior segment of the lateral sulcus	2.49(0.27)	2.54(0.32)	2.50(0.28)	0.768(.445)	0.197(.845)	−0.500(.619)
40	R Vertical ramus of the anterior segment of the lateral sulcus	2.64(0.40)	2.63(0.35)	2.52(0.31)	−0.207(.837)	−1.476(.143)	−1.235(.221)
41	R Posterior ramus (or segment) of the lateral sulcus	2.63(0.20)	2.61(0.20)	2.61(0.20)	−0.462(.645)	−0.501(.618)	−0.032(.975)
42	R Occipital pole	1.91(0.16)	1.96(0.17)	2.04(0.28)	1.389(.168)	2.775(.007)	1.333(.188)
43	R Temporal pole	2.40(0.35)	2.45(0.34)	2.49(0.38)	0.651(.517)	1.073(.286)	0.392(.696)
44	R Calcarine sulcus	2.02(0.15)	2.05(0.20)	2.09(0.16)	0.802(.425)	1.804(.075)	0.664(.509)
45	R Central sulcus	1.96(0.13)	1.90(0.11)	1.95(0.17)	−1.907(.060)	−0.091(.928)	1.385(.171)
46	R Marginal branch (or part) of the cingulate sulcus	2.52(0.20)	2.54(0.20)	2.50(0.15)	0.269(.788)	−0.524(.601)	−0.744(.460)
47	R Anterior segment of the circular sulcus of the insula	2.90(0.29)	2.87(0.32)	2.85(0.39)	−0.328(.744)	−0.696(.488)	−0.313(.755)
48	R Inferior segment of the circular sulcus of the insula	2.70(0.27)	2.70(0.24)	2.73(0.22)	−0.095(.925)	0.530(.598)	0.591(.557)
49	R Superior segment of the circular sulcus of the insula	2.78(0.19)	2.76(0.23)	2.73(0.25)	−0.425(.672)	−1.037(.303)	−0.478(.634)
50	R Anterior transverse collateral sulcus	2.53(0.22)	2.53(0.25)	2.47(0.33)	−0.059(.953)	−1.028(.307)	−0.767(.446)
51	R Posterior transverse collateral sulcus	2.24(0.23)	2.25(0.28)	2.29(0.26)	0.187(.852)	0.823(.413)	0.499(.620)
52	R Inferior frontal sulcus	2.41(0.19)	2.44(0.19)	2.45(0.14)	0.790(.432)	0.992(.324)	0.122(.903)
53	R Middle frontal sulcus	2.27(0.19)	2.30(0.23)	2.43(0.25)	0.601(.550)	3.242(.002)	2.099(.040)

https://doi.org/10.1017/S0954579418000093 Published online by Cambridge University Press

Table 5 (*cont.*)

No.	Area	CONT	MALT	PTSD	MALT vs. CONT	PTSD vs. CONT	PTSD vs. MALT
		mean(*SD*)			*t*(*p*)		
54	R Superior frontal sulcus	2.44(0.20)	2.35(0.20)	2.44(0.22)	−2.065(.042)	−0.104(.917)	1.641(.106)
55	R Sulcus intermedius primus (of Jensen)	2.46(0.21)	2.46(0.22)	2.50(0.24)	−0.013(.990)	0.684(.496)	0.594(.555)
56	R Intraparietal sulcus (interparietal sulcus) and transverse parietal sulci	2.38(0.15)	2.35(0.21)	2.38(0.16)	−0.624(.534)	0.009(.993)	0.533(.596)
57	R Middle occipital sulcus and lunatus sulcus	2.22(0.20)	2.28(0.23)	2.26(0.21)	1.312(.193)	0.906(.367)	−0.369(.713)
58	R Superior occipital sulcus and transverse occipital sulcus	2.28(0.19)	2.31(0.21)	2.34(0.15)	0.648(.519)	1.558(.123)	0.723(.472)
59	R Anterior occipital sulcus and preoccipital notch	2.50(0.17)	2.52(0.16)	2.56(0.18)	0.372(.711)	1.492(.139)	1.015(.314)
60	R Lateral occipito-temporal sulcus	2.67(0.21)	2.70(0.26)	2.64(0.22)	0.535(.594)	−0.696(.488)	−0.990(.326)
61	R Medial occipito-temporal sulcus (collateral sulcus) and lingual sulcus	2.52(0.18)	2.52(0.18)	2.51(0.20)	0.062(.950)	−0.303(.763)	−0.318(.752)
62	R Lateral orbital sulcus	2.29(0.26)	2.41(0.29)	2.41(0.30)	1.906(.060)	2.008(.048)	0.095(.925)
63	R Medial orbital sulcus	2.27(0.24)	2.30(0.21)	2.27(0.24)	0.609(.544)	−0.038(.970)	−0.600(.551)
64	R Orbital sulci (H-shaped sulci)	2.79(0.22)	2.80(0.26)	2.84(0.28)	0.171(.864)	1.034(.304)	0.688(.494)
65	R Parieto-occipital sulcus (or fissure)	2.42(0.24)	2.41(0.27)	2.39(0.20)	−0.176(.861)	−0.724(.471)	−0.436(.664)
66	R Pericallosal sulcus	2.15(0.25)	2.23(0.31)	2.19(0.29)	1.324(.189)	0.708(.481)	−0.507(.614)
67	R Postcentral sulcus	2.33(0.21)	2.28(0.19)	2.32(0.16)	−0.936(.352)	−0.171(.865)	0.798(.428)
68	R Inferior part of the precentral sulcus	2.58(0.16)	2.57(0.19)	2.57(0.20)	−0.443(.659)	−0.192(.848)	0.197(.844)
69	R Superior part of the precentral sulcus	2.37(0.19)	2.28(0.19)	2.31(0.21)	−2.158(.034)	−1.466(.146)	0.580(.564)
70	R Suborbital sulcus	2.77(0.49)	2.79(0.46)	2.86(0.45)	0.187(.852)	0.820(.414)	0.577(.566)
71	R Subparietal sulcus	2.69(0.21)	2.66(0.20)	2.62(0.19)	−0.600(.550)	−1.620(.109)	−0.908(.368)
72	R Inferior temporal sulcus	2.60(0.20)	2.67(0.23)	2.63(0.18)	1.344(.183)	0.687(.494)	−0.658(.513)
73	R Superior temporal sulcus	2.76(0.14)	2.78(0.19)	2.76(0.15)	0.560(.577)	0.191(.849)	−0.322(.749)
74	R Transverse temporal sulcus	2.65(0.26)	2.61(0.35)	2.80(0.29)	−0.579(.564)	2.454(.016)	2.295(.025)

Note: Between-group comparisons were based on independent *t* tests without correction. Area numbers and names were according to Destrieux et al. (2010). CONT, nonmaltreated controls; MALT, maltreated youth without PTSD; PTSD, maltreated youth with PTSD.

PCC as a node in the brain network that connects to other areas and/or regulates neurocommunications in maltreated youth with chronic PTSD. These findings, as well as our results, suggest that the PCC and its role in the posterior brain network contribute to the symptoms of pediatric maltreatment-related PTSD.

We also found that maltreated youth with PTSD versus those without PTSD showed smaller centrality in the left ACC. This result is consistent with a previous finding (Mueller et al., 2015) demonstrating that veterans with PTSD exhibited smaller degree centrality in the left ACC, suggesting that the smaller centrality in the left ACC appears in both pediatric PTSD and adult PTSD. The ACC has been widely reported in studies of attention, emotion regulation, and inhibitory control, and PTSD (for review see Hughes & Shin, 2011). Reduced activations in response to combat-related words were detected in veterans with PTSD (Shin et al., 2001). Smaller gray matter volume was found in the ACC in victims with PTSD compared with those without PTSD (Yamasue et al., 2003). Smaller negative correlations between the amygdala and ACC were also reported in male veterans with PTSD than combat controls (Sripada et al., 2012). Our finding provided new insight into the roles of the ACC in PTSD through the structural covariance network approach, suggesting the reduced importance of the ACC in regulating neural communication in the brain network of maltreated youth with versus those resilient to PTSD. Although we did not see any significant differences in cingulate cortical thickness, this finding of smaller centrality in the left ACC appears in both pediatric PTSD and adult PTSD (Mueller et al., 2015) and may be one of the first developmental markers to show poor outcome in maltreated youth. Smaller centrality in the left ACC was seen in young adults exposed to maltreatment compared to unexposed controls (Teicher et al., 2014). However, we did not find between-group differences involving nonmaltreated controls in the ACC. Future longitudinal investigations are needed to uncover the role of the ACC in the brain network of youth who experience maltreatment and those who experience pediatric maltreatment-related PTSD.

Our study provides support for the fact that smaller centrality in the right IFC brain nodes are uniquely affected by maltreatment. Maltreated youth without PTSD showed smaller centrality in the right IFC than nonmaltreated controls, and maltreated youth with PTSD showed even smaller centrality in the right IFC than those without PTSD. These results suggest the specific role of the right IFC in childhood maltreatment and pediatric maltreatment-related PTSD. In other words, low centrality in the right IFC represents experiencing

https://doi.org/10.1017/S0954579418000093 Published online by Cambridge University Press

maltreatment and the lowest centrality in this area signals pediatric maltreatment-related PTSD. The right IFC has been shown to play critical roles in networks that control inhibition (for a review, see Hampshire, Chamberlain, Monti, Duncan, & Owen, 2010) and emotion regulation (Etkin, Buchel, & Gross, 2015; Wager, Davidson, Hughes, Lindquist, & Ochsner, 2008). Maltreated children performed more poorly on inhibitory control (Cowell, Cicchetti, Rogosch, & Toth, 2015) and emotional regulation (Kim & Cicchetti, 2010) tasks and behaviors than controls. PTSD was also accompanied by impaired fear inhibition (Jovanovic et al., 2010), and difficulty in regulating negative emotions (Shepherd & Wild, 2014). Adolescents and young adults who experienced physical and sexual abuse exhibited reduced cortical thickness in areas including the inferior frontal gyrus (Gold et al., 2016). However, not all studies agree, as one study of younger youth showed increased gray matter density mainly localized to the ventral prefrontal cortex in youth with PTSD and subthreshold PTSD compared to nontraumatized control youth (Carrion et al., 2009). Our previous work (Crozier, Wang, Huettel, & De Bellis, 2014) showed that maltreated males exhibited smaller activation in the inferior frontal gyrus compared to control males when performing an emotional oddball task involving detecting targets with fear face distractors. A recent study (van Rooij et al., 2014) also detected reduced activations in the right inferior frontal gyrus response during proactive inhibition in PTSD subjects compared to combat controls. Lower centrality may reflect less important roles of the inferior frontal gyrus as a node in controlling network information transfer and neural communication (He et al., 2008). In line with this thought and previous findings, our results suggest weakened roles of the right IFC in the brain network employed for the control of inhibition and emotional regulation in maltreated youth with and without PTSD.

Maltreatment was also associated with centrality differences in the left PCC. Smaller centralities in the left PCC (subparietal sulcus) were detected in maltreated youth with and without PTSD compared to nonmaltreated controls. A few previous studies have reported the functional dissociations between the left and right PCC. The left PCC is involved in networks that control working memory, attention, spatial memory (Cabeza & Nyberg, 2000), and autobiographical memory retrieval (Maddock, Garrett, & Buonocore, 2008). Maltreated youth with and without PTSD show deficits in working memory and attention (De Bellis, Woolley, & Hooper, 2013). Our findings may suggest an interesting difference between the left and right PCC that may be related to the wide range of attentional and memory problems commonly seem in maltreated youth.

A previous study (Mueller et al., 2015) showed that veterans with PTSD versus controls exhibited larger betweenness centrality in the left insula (in the entire cortical network), which is closely connected to the IFC. Our research did not support this finding. A possible explanation for the inconsistency is that age mediates the effects of maltreatment-related PTSD on structural covariance network. The participants in our study were youth (age 6.2–16.2 years) whose brains were still developing (Shaw et al., 2008), whereas the prior studies investigated veterans (age above 22 years) who may also have suffered age-related gray matter atrophy (Mueller et al., 2015).

Resilience to PTSD following maltreatment was associated with centrality differences in the right FP (transverse frontopolar gyri and sulci) and the left ACC. Maltreated youth without PTSD exhibited larger centrality in this area than the other two groups. The transverse frontopolar gyri and sulci is a complex structure involved in networks that control the efficient episodic memory processing (Fleischman et al., 2014), error recognition (Li, Yan, Bergquist, & Sinha, 2007), and shows strong connections to the brain areas involved in the anterior DMN, including the networks that involve the ACC, medial prefrontal cortex, orbitofrontal cortex, temporal pole, and amygdala (Liu et al., 2013). Moreover, the larger centralities in the FP and ACC may reflect their more important roles in the networks that involve cognitive control over affective processing. This better cognitive control may be responsible for the higher levels of global function in the group resilient to PTSD compared to those with PTSD. Although previous structural covariance analyses on maltreatment and PTSD did not report findings in the FP, recent studies revealed the linkage between this area and PTSD symptoms; Sadeh et al. (2015) found that smaller frontopolar cortical thickness at higher levels of PTSD symptoms were accompanied with commission errors in a Go/No-Go task with emotional stimuli. In a later study, Sadeh et al. (2016) showed that PTSD symptom severity negatively correlated with frontopolar cortical thickness and positively correlated with the methylation of the spindle and kinetochore-associated complex subunit 2 (SKA2) gene. All of these findings suggested that optimal functioning of the FP plays a critical role in protecting against developing PTSD following maltreatment. More studies are required to investigate the precise roles of the FP, which may to be a target for PTSD clinical intervention.

Limitations

This study had several strengths including study design, which included medically healthy maltreated participants without prenatal substance exposure or personal history of substance use disorder, and who had full-scale IQs within the typical developmental range. However, there are several limitations inherent to cortical thickness covariance network analyses. First, our analysis was based on the large-scale covariance of cortical thickness. We were not able to examine subcortical regions such as the amygdala and hippocampus. Second, this method does not allow us to examine the role of individual differences on network characteristics, given that only one network is formed and one set of network measures may be calculated per group. Because we do not know the individual centrality values within each group, we cannot perform additional correlation analyses between centrality and number of PTSD symptoms. This is an inherent limitation in these types of analyses. Third, our study utilized a cross-sectional design, which limits

https://doi.org/10.1017/S0954579418000093 Published online by Cambridge University Press

inferences about the causal relationships between maltreatment, PTSD status, and brain cortical thickness-based structural covariance network. In addition, we controlled for potentially confounding sociodemographic covariates that may have led to a higher rate of false negative results. However, these variables did not show significant between-group differences in this study design; including them as co-variates in the statistical model was unlikely to reduce the statistical power of this study's regions of interest analyses (Miller & Chapman, 2001). Fourth, we also note that resilience to PTSD does not mean invulnerability to trauma. The term "resilient" in the literature is typically defined as not having a particular pathology (Kaufman, Cook, et al., 1994). The maltreated group without PTSD were resilient to chronic and persistent PTSD and its associated comorbidities (e.g., depression and externalizing disorders), but they were not invulnerable (De Bellis et al., 2015; Morey et al., 2016). The level of function on the Children Global Assessment Scale scores in the PTSD group (mean 55) was in the range of symptoms causing serious impairment in most areas and requiring treatment; while the Children Global Assessment Scale scores in the maltreated group without PTSD (mean 67.8) is in the range of variable functioning with difficulties in some but not all social areas and may only be apparent in a dysfunctional setting. Number of traumatic events, chronic traumas, or maltreatment types probably did not influence our results, as both maltreatment groups suffered a mean of at least five maltreatment types, putting both groups at extremely high risk for adolescent and adult psychopathology and health risk behaviors associated with the leading causes of death in adulthood (Dube, Felitti, Dong, Giles, & Anda, 2003; Felitti et al., 1998). However, our study raises questions about the nature of allostatic load and individual vulnerability (as opposed to resilience) to chronic PTSD in maltreated children and adolescents. Does a specific threshold of maltreatment exist for each individual, above which all maltreated youth are vulnerable to chronic PTSD and will be found to have larger centrality in the right PCC (negatively affecting networks that control self-referential processing) and smaller centrality in right IFC (negatively affecting networks that control inhibition and emotional regulation) compared to nontraumatized youth? Given that this investigation is cross-sectional, we cannot answer this question. The lack of published longitudinal studies in maltreated youth is an impediment in formulating an answer and is a vital area for future research.

Conclusion

Here, we provided novel findings of difference between maltreated youth with and without chronic PTSD and healthy control subjects, filling the gap in the developmental literature by studying a stress-related condition that has previously only been investigated in adults exposed to childhood maltreatment (Teicher et al., 2014). This advances the field by demonstrating that network centrality differences are evident in childhood PTSD, early in the life course of its development. Our study demonstrated cortical thickness-based structural covariance network differences both in networks unique to maltreated youth with chronic PTSD and those resilient to chronic PTSD following maltreatment. These brain structures are also associated with the successful attainment of age-appropriate social cognition, attention, emotional processing, and inhibitory control. Future studies are needed to elucidate the relationships between brain network attributes, symptoms, cognitive, and behavioral performance in traumatized youth. Beyond the domain of brain research, network analysis also makes it possible to identify "central" symptoms having a large influence over other PTSD symptoms and can be significant targets for research and treatment. A recently published study by Russell, Neill, Carrion, and Weems (2017) showed that PTSD can be represented by a graph indicating relationships between PTSD symptoms and age, and how the important symptoms within the network vary across childhood and adolescence. Future large-scale multisite longitudinal studies investigating age, PTSD symptoms, along with brain networks in maltreated youth should help fill these gaps as well as the mechanisms of how our findings relate to chronic PTSD and its associated disability. In addition, it would inform the field of factors that influence better outcomes (resilience to chronic PTSD despite severe trauma).

References

Boersma, M., Smit, D. J. A., de Bie, H. M. A., Van Baal, G. C. M., Boomsma, D. I., de Geus, E. J. C., . . . Stam, C. J. (2011). Network analysis of resting state EEG in the developing young brain: Structure comes with maturation. *Human Brain Mapping*, *32*, 413–425.

Bremner, J. D., Narayan, M., Staib, L., Southwick, S. M., McGlashan, T., & Charney, D. S. (1999). Neural correlates of memories of childhood sexual abuse in women with and without posttraumatic stress disorder. *American Journal of Psychiatry*, *156*, 1787–1795.

Cabeza, R., & Nyberg, L. (2000). Imaging cognition II: An empirical review of 275 PET and fMRI studies. *Journal of Cognitive Neuroscience*, *12*, 1–47.

Carrion, V. G., Weems, C. F., Watson, C., Eliez, S., Menon, V., & Reiss, A. L. (2009). Converging evidence for abnormalities of the prefrontal cortex and evaluation of midsagittal structures in pediatric posttraumatic stress disorder: An MRI study. *Psychiatry Research: Neuroimaging*, *172*, 226–234.

Cowell, R. A., Cicchetti, D., Rogosch, F. A., & Toth, S. L. (2015). Childhood maltreatment and its effect on neurocognitive functioning: Timing and chronicity matter. *Development and Psychopathology*, *27*, 521–533.

Crozier, J. C., Wang, L., Huettel, S. A., & De Bellis, M. D. (2014). Neural correlates of cognitive and affective processing in maltreated youth with posttraumatic stress symptoms: Does gender matter? *Development and Psychopathology*, *26*, 491–513.

De Bellis, M. D. (2001). Developmental traumatology: The psychobiological development of maltreated children and its implications for research, treatment, and policy. *Development and Psychopathology*, *13*, 539–564. doi:10.1017/S0954579401003078.

De Bellis, M. D., Hooper, S. R., Chen, S. D., Provenzale, J. M., Boyd, B. D., Glessner, C. E., . . . Woolley, D. P. (2015). Posterior structural brain volumes differ in maltreated youth with and without chronic posttraumatic stress disorder. *Development and Psychopathology*, *27*, 1555–1576. doi:10.1017/S0954579415000942.

De Bellis, M. D., Hooper, S., Spratt, E. G., & Woolley, D. W. (2009). Neuropsychological findings in childhood neglect and their relationships to pediatric PTSD. *Journal of the International Neuropsychological Society*, *15*, 868–878.

De Bellis, M., & Kuchibhatla, M. (2006). Cerebellar volumes in pediatric maltreatment-related posttraumatic stress disorder. *Biological Psychiatry*, *60*, 697–703.

De Bellis, M. D., Keshavan, M. S., Clark, D. B., Casey, B. J., Giedd, J. N., Boring, A. M., . . . Ryan, N. D. (1999). A.E. Bennett Research Award. Developmental traumatology. Part II: Brain development. *Biological Psychiatry*, *45*, 1271–1284.

De Bellis, M. D., Woolley, D. P., & Hooper, S. R. (2013). Neuropsychological findings in pediatric maltreatment: Relationship of PTSD, dissociative symptoms, and abuse/neglect indices to neurocognitive outcomes. *Child Maltreatment*, *18*, 171–183. doi:10.1177/1077559513497420.

De Bellis, M. D., & Zisk, A. (2014). The biological effects of childhood trauma. *Child and Adolescent Psychiatric Clinics of North America*, *23*, 185–222. doi:10.1016/j.chc.2014.01.002.

Destrieux, C., Fischl, B., Dale, A., & Halgren, E. (2010). Automatic parcellation of human cortical gyri and sulci using standard anatomical nomenclature. *Neuroimage*, *53*, 1–15. doi:10.1016/j.neuroimage.2010.06.010.

Di Martino, A., Fair, D. A., Kelly, C., Satterthwaite, T. D., Castellanos, F. X., Thomason, M. E., . . . Milham, M. P. (2014). Unraveling the miswired connectome: A developmental perspective. *Neuron*, *83*, 1335–1353. doi:10.1016/j.neuron.2014.08.050.

Dube, S. R., Felitti, V. J., Dong, M., Giles, W. H., & Anda, R. F. (2003). The impact of adverse childhood experiences on health problems: Evidence from four birth cohorts dating back to 1900. *Pediatrics*, *37*, 268–277.

Efron, B., & Tibshirani, R. (1993). *An introduction to the bootstrap*. New York: Chapman & Hall.

Etkin, A., Buchel, C., & Gross, J. J. (2015). The neural bases of emotion regulation. *Nature Reviews Neuroscience*, *16*, 693–700.

Fair, D. A., Cohen, A. L. Dosenbach, N. U. F., Church, J. A., Miezin, F. M., Barch, D. M., . . . Schlaggar, B. L. (2008). The maturing architecture of the brain's default network. *Proceedings of the National Academy of Sciences USA*, *105*, 4028–4032.

Felitti, V. J., Anda, R. F., Nordenberg, D., Williamson, D. F., Spitz, A. M., Edwards, V., . . . Marks, J. S. (1998). Relationship of childhood abuse and household dysfunction to many of the leading causes if death in adults. *American Journal of Preventive Medicine*, *14*, 245–258.

Fleischman, D. A., Leurgans, S., Arfanakis, K., Arvanitakis, Z., Barnes, L. L., Boyle, P. A., . . . Bennett, D. A. (2014). Gray-matter macrostructure in cognitively healthy older persons: Associations with age and cognition. *Brain Structure and Function*, *219*, 2029–2049.

Fox, M. D., Snyder, A. Z., Vincent, J. L., Corbetta, M., Van Essen, D. C., & Raichle, M. E. (2005). The human brain is intrinsically organized into dynamic, anticorrelated functional networks. *Proceedings of the National Academy of Sciences of the USA*, *102*, 9673–9678.

Gold, A. L., Sheridan, M. A., Peverill, M., Busso, D. S., Lambert, H. K., Alves, S., . . . K. A. (2016). Childhood abuse and reduced cortical thickness in brain regions involved in emotional processing. *Journal of Child Psychology and Psychiatry*, *57*, 1154–1164. doi:10.1111/jcpp.12630.

Gong, G. L., He, Y., Chen, Z. J., & Evans, A. C. (2012). Convergence and divergence of thickness correlations with diffusion connections across the human cerebral cortex. *Neuroimage*, *59*, 1239–1248. doi:10.1016/j.neuroimage.2011.08.017.

Gong, Q. Y., Li, L. J., Du, M. Y., Pettersson-Yeo, W., Crossley, N., Yang, X., . . . Mechelli, A. (2014). Quantitative prediction of individual psychopathology in trauma survivors using resting-state fMRI. *Neuropsychopharmacology*, *39*, 681–687. doi:10.1038/npp.2013.251.

Hampshire, A., Chamberlain, S. R., Monti, M. M., Duncan, J., & Owen, A. M. (2010). The role of the right inferior frontal gyrus: Inhibition and attentional control. *Neuroimage*, *50*, 1313–1319.

He, Y., Chen, Z. J., & Evans, A. C. (2007). Small-world anatomical networks in the human brain revealed by cortical thickness from MRI. *Cerebral Cortex*, *17*, 2407–2419. doi:10.1093/cercor/bhl149.

He, Y., Chen, Z., & Evans, A. (2008). Structural insights into aberrant topological patterns of large-scale cortical networks in Alzheimer's Disease. *Journal of Neuroscience*, *28*, 4756–4766. doi:10.1523/Jneurosci.0141-08.2008.

He, Y., Dagher, A., Chen, Z., Charil, A., Zijdenbos, A., Worsley, K., & Evans, A. (2009). Impaired small-world efficiency in structural cortical networks in multiple sclerosis associated with white matter lesion load. *Brain*, *132*, 3366–3379.

He, Y., & Evans, A. (2010). Graph theoretical modeling of brain connectivity. *Current Opinion in Neurology*, *23*, 341–350. doi:10.1097/WCO.0-b013e32833aa567.

Hofer, S., & Frahm, J. (2006). Topography of the human corpus callosum revisited—Comprehensive fiber tractography using diffusion tensor magnetic resonance imaging. *Neuroimage*, *32*, 989–994.

Hughes, K. C., & Shin, L. M. (2011). Functional neuroimaging studies of post-traumatic stress disorder. *Expert Review of Neurotherapeutics*, *11*, 275–285.

Hussey, J. M., Chang, J. J., & Kotch, J. B. (2006). Child maltreatment in the United States: Prevalence, risk factors, and adolescent health consequences. *Pediatrics*, *118*, 933–942.

Jovanovic, T., Norrholm, S. D., Blanding, N. Q., Davis, M., Duncan, E., Bradley, B., & Ressler, K. J. (2010). Impaired fear inhibition is a biomarker of PTSD but not depression. *Depression and Anxiety*, *27*, 244–251.

Kaufman, J., Birmaher, B., Brent, D., Rao, U., Flynn, C., Moreci, P., . . . Ryan, N. (1997). Schedule for Affective Disorders and Schizophrenia for School-Age Children—Present and Lifetime Version (K-SADS-PL): Initial reliability and validity data. *Journal of the American Academy of Child and Adolescent Psychiatry*, *36*, 980–988.

Kaufman, J., Cook, A., Arny, L., Jones, B., & Pittinsky, T. (1994). Problems defining resiliency: Illustrations from the study of maltreated children. *Development and Psychopathology*, *6*, 215–229.

Kaufman, J., Jones, B., Stieglitz, E., Vitulano, L., & Mannarino, A. (1994). The use of multiple informants to assess children's maltreatment experiences. *Journal of Family Violence*, *9*, 227–248.

Kim, J., & Cicchetti, D. (2010). Longitudinal pathways linking child maltreatment, emotion regulation, peer relations, and psychopathology. *Journal of Child Psychology and Psychiatry*, *51*, 706–716.

Leech, R., & Sharp, D. J. (2014). The role of the posterior cingulate cortex in cognition and disease. *Brain*, *137*, 12–32. doi:10.1093/brain/awt162.

Leslie, L. K., Gordon, J. N., Meneken, L., Premji, K., Michaelmore, K. L., & Ganger, W. (2005). The physical, developmental, and mental health needs of young children in child welfare by initial placement type. *Developmental and Behavioral Pediatrics*, *26*, 177–185.

Li, C.-S. R., Yan, P., Bergquist, K. L., & Sinha, R. (2007). Greater activation of the "default" brain regions predicts stop signal errors. *Neuroimage*, *38*, 640–648.

Liu, H. G., Qin, W., Li, W., Fan, L. Z., Wang, J. J., Jiang, T. Z., & Yu, C. S. (2013). Connectivity-based parcellation of the human frontal pole with diffusion tensor imaging. *Journal of Neuroscience*, *33*, 6782–6790. doi:10.1523/Jneurosci.4882-12.2013.

Maddock, R. J., Garrett, A. S., & Buonocore, M. H. (2008). Remembering familiar people: The posterior cingulate cortex and autobiographical memory retrieval. *Neuroscience*, *104*, 667–676.

Miller, G. A., & Chapman, J. P. (2001). Misunderstanding analysis of covariance. *Journal of Abnormal Psychology*, *110*, 40–48. doi:10.1037//0021-843x.110.1.40.

Morey, R. A., Haswell, C. C., Hooper, S. R., & De Bellis, M. D. (2016). Amygdala, hippocampus, and ventral medial prefrontal cortex volumes differ in maltreated youth with and without chronic posttraumatic stress disorder. *Neuropsychopharmacology*, *41*, 791–801. doi:10.1038/npp.2015.205.

Mueller, S. G., Ng, P., Neylan, T., Mackin, S., Wolkowitz, O., Mellon, S., . . . Weiner, M. W. (2015). Evidence for disrupted gray matter structural connectivity in posttraumatic stress disorder. *Psychiatry Research: Neuroimaging*, *234*, 194–201. doi:10.1016/j.pscychresns.2015.09.006.

Perez, C. M., & Widom, C. S. (1994). Childhood victimization and long-term intellectual and academic outcomes. *Child Abuse & Neglect*, *18*, 617–633. doi:10.1016/0145-2134(94)90012-4.

Pfefferbaum, A., Rohlfing, T., Pohl, K. M., Lane, B., Chu, W., Kwon, D., . . . Sullivan, E. V. (2015). Adolescent development of cortical and white matter structure in the NCANDA sample: Role of sex, ethnicity, puberty, and alcohol drinking. *Cerebral Cortex*, *26*, 4101–4121. doi:10.1093/cercor/bhv205.

Raffelt, D. A., Tournier, J. D., Smith, R. E., Vaughan, D. N., Jackson, G., Ridgway, G. R., & Connelly, A. (2017). Investigating white matter fibre density and morphology using fixel-based analysis. *Neuroimage*, *144*, 58–73.

Raghavan, R., Zima, B. T., Andersen, R. M., Leibowitz, A. A., Schuster, M. A., & Landsverk, J. (2005). Psychotropic medication use in a national probability sample of children in the child welfare system. *Journal of Child and Adolescent Psychopharmacology*, *15*, 97–106.

Rubinov, M., & Sporns, O. (2010). Complex network measures of brain connectivity: Uses and interpretations. *Neuroimage*, *52*, 1059–1069. doi:10.1016/j.neuroimage.2009.10.003.

Russell, J. D., Neill, E. L., Carrion, V. G., & Weems, C. F. (2017). The network structure of posttraumatic stress symptoms in children and adolescents exposed to disasters. *Journal of the American Academy of Child & Adolescent Psychiatry*, *56*, 669–677.

Sadeh, N., Spielberg, J. M., Logue, M. W., Wolf, E. J., Smith, A. K., Lusk, J., . . . Miller, M. W. (2016). SKA2 methylation is associated with decreased prefrontal cortical thickness and greater PTSD severity among trauma-exposed veterans. *Molecular Psychiatry*, *21*, 357–363. doi:10.1038/mp.2015.134.

Sadeh, N., Spielberg, J. M., Miller, M. W., Milberg, W. P., Salat, D. H., Amick, M. M., . . . McGlinchey, R. E. (2015). Neurobiological indicators of disinhibition in posttraumatic stress disorder. *Human Brain Mapping*, *36*, 3076–3086. doi:10.1002/hbm.22829.

Shaffer, D., Gould, M. S., Brasic, J., Ambrosini, P., Fisher, P., Bird, H., & Aluwahlia, S. (1983). A Children's Global Assessment Scale. *Archives of General Psychiatry*, *40*, 1228–1231.

Shaw, P., Kabani, N. J., Lerch, J. P., Eckstrand, K., Lenroot, R., Gogtay, N., . . . Wise, S. P. (2008). Neurodevelopmental trajectories of the human cerebral cortex. *Journal of Neuroscience*, *28*, 3586–3594. doi:10.1523/Jneurosci.5309-07.2008.

Shepherd, L., & Wild, J. (2014). Emotion regulation, physiological arousal and PTSD symptoms in trauma-exposed individuals. *Journal of Behavior Therapy and Experimental Psychiatry*, *45*, 360–367.

Shin, L. M., Whalen, P. J., Pitman, R. K., Bush, G., Macklin, M. L., Lasko, N. B., . . . Rauch, S. L. (2001). An fMRI study of anterior cingulate function in posttraumatic stress disorder. *Biological Psychiatry*, *50*, 932–942. doi:10.1016/S0006-3223(01)01215-X.

Smith, D. K., Johnson, A. B., Pears, K. C., Fisher, P. A., & DeGarmo, D. S. (2007). Child maltreatment and foster care: Unpacking the effects of prenatal and postnatal parental substance use. *Child Maltreatment*, *12*, 150–160. doi:10.1177/1077559507300129.

Sripada, R. K., King, A. P., Welsh, R. C., Garfinkel, S. N., Wang, X., Sripada, C. S., & Liberzon, I. (2012). Neural dysregulation in posttraumatic stress disorder: Evidence for disrupted equilibrium between salience and default mode brain networks. *Psychosomatic Medicine*, *74*, 904–911. doi:10.1097/PSY.0b013e318273bf33.

Supekar, K., Uddin, L. Q., Prater, K., Amin, H., Greicius, M. D., & Menon, V. (2010). Development of functional and structural connectivity within the default mode network in young children. *Neuroimage*, *52*, 290–301.

Teicher, M. H., Anderson, C. M., Ohashi, K., & Polcari, A. (2014). Childhood maltreatment: Altered network centrality of cingulate, precuneus, temporal pole and insula. *Biological Psychiatry*, *76*, 297–305. doi:10.1016/j.biopsych.2013.09.016.

Teicher, M. H., Samson, J. A., Anderson, C. M., & Ohashi, K. (2016). The effects of childhood maltreatment on brain structure, function and connectivity. *Nature*, *17*, 652–666.

Utevsky, A. V., Smith, D. V., & Huettel, S. A. (2014). Precuneus is a functional core of the default-mode network. *Journal of Neuroscience*, *34*, 932–940.

van Rooij, S. J. H., Rademaker, A. R., Kennis, M., Vink, M., Kahn, R. S., & Geuze, E. (2014). Impaired right inferior frontal gyrus response to contextual cues in male veterans with PTSD during response inhibition. *Journal of Psychiatry and Neuroscience*, *39*, 330–338. doi:10.1503/jpn.130223.

van Straaten, E. C. W., & Stam, C. J. (2012). Structure out of chaos: Functional brain network analysis with EEG, MEG, and functional MRI. *European Neuropsychopharmacology*, *23*, 7–18.

Wager, T. D., Davidson, M. L., Hughes, B. L., Lindquist, M. A., & Ochsner, K. N. (2008). Prefrontal-subcortical pathways mediating successful emotion regulation. *Neuron*, *59*, 1037–1050.

Wechsler, D. (1991). *Wechsler Intelligence Scale for Children* (3rd ed.). San Antonio: Psychological Corporation.

Winkler, A. M., Webster, M. A., Vidaurre, D., Nichols, T. E., & Smith, S. M. (2015). Multi-level block permutation. *Neuroimage*, *123*, 253–268. doi:10.1016/j.neuroimage.2015.05.092.

Yamasue, H., Kasai, K., Iwanami, A., Ohtani, T., Yamada, H., Abe, O., . . . Kato, N. (2003). Voxel-based analysis of MRI reveals anterior cingulate gray-matter volume reduction in posttraumatic stress disorder due to terrorism. *Proceedings of the National Academy of Sciences of the USA*, *100*, 9039–9043.

Zalesky, A., Fornito, A., & Bullmore, E. T. (2010). Network-based statistic: Identifying differences in brain networks. *Neuroimage*, *53*, 1197–1207. doi:10.1016/j.neuroimage.2010.06.041.

Zhou, Y., Wang, Z., Qin, L. D., Wan, J. Q., Sun, Y. W., Su, S. S., . . . Xu, J. R. (2012). Early altered resting-state functional connectivity predicts the severity of post-traumatic stress disorder symptoms in acutely traumatized subjects. *PLOS ONE*, *7*, e46833.